

Fast Performance Uncertainty Estimation via Pushover and Approximate IDA[‡]

Michalis Fragiadakis^{1,*},[†], Dimitrios Vamvatsikos²

¹ School of Civil Engineering, National Technical University of Athens, Greece

Department of Civil Engineering, University of Thessaly, Volos, Greece

² Department of Civil and Environmental Engineering, University of Cyprus, Nicosia 1678, Cyprus

SUMMARY

Approximate methods based on the static pushover are introduced to estimate the seismic performance uncertainty of structures having non-deterministic modeling parameters. At their basis lies the use of static pushover analysis to approximate Incremental Dynamic Analysis (IDA) and estimate the demand and capacity epistemic uncertainty. As a testbed we use a nine-storey steel frame having beam hinges with uncertain moment-rotation relationships. Their properties are fully described by six, randomly distributed, parameters. Using Monte Carlo simulation with latin hypercube sampling, a characteristic ensemble of structures is created. The Static Pushover to IDA (SPO2IDA) software is used to approximate the IDA capacity curve from the appropriately post-processed results of the static pushover. The approximate IDAs allow the evaluation of the seismic demand and capacity for the full range of limit-states, even close to global dynamic instability. Moment estimating techniques such as Rosenblakth's point estimating method and the first-order, second-moment (FOSM) method are adopted as simple alternatives to obtain performance statistics with only a few simulations. The pushover is shown to be a tool that combined with SPO2IDA and moment estimating techniques can supply the uncertainty in the seismic performance of first-mode dominated buildings for the full range of limit-states, thus replacing semi-empirical or code tabulated values (e.g. FEMA-350), often adopted in performance-based earthquake engineering. Copyright © 2009 John Wiley & Sons, Ltd.

KEY WORDS: Epistemic Uncertainty; Static Pushover Analysis; Incremental Dynamic Analysis; Simulation; Moment estimating methods; performance-based earthquake engineering.

1. INTRODUCTION

Structural analysis is plagued by both aleatory randomness, e.g. natural ground motion record variability, and epistemic uncertainty, stemming from modeling assumptions or errors. Design codes recognize the importance of uncertainty in the process of seismic design by

*Correspondence to: Michalis Fragiadakis, Iroon Polutexneiou St., Zografou 15780, Athens, Greece.

[†]E-mail: mfrag@mail.ntua.gr

[‡]Based on a short paper presented at the 14th World Conference on Earthquake Engineering, Beijing, China, 2008.

implicitly including generic safety factors in the model, the material properties and the loads. Unfortunately little data is available on the seismic demand and capacity epistemic uncertainty, an issue that is ultimately dealt with tabulated values. Epistemic uncertainty usually receives little attention due to the inherent difficulties and the computational cost in estimating it. Since both randomness and uncertainty are important factors in performance-based earthquake engineering, efficient estimation methods are always desirable.

Perhaps the first guideline that explicitly treats uncertainty in seismic design is FEMA-350 (SAC/FEMA 2000 [1]). The SAC/FEMA project caused the widespread adoption of the notion of uncertainty in earthquake engineering applications, and became a major motivation to study rational ways to include the uncertainty in performance estimation. Cornell *et al.* [2] formed the background of the SAC/FEMA approach for the probabilistic assessment of steel frames which allows the inclusion of epistemic uncertainties simply by considering the dispersion they cause on the median demand and capacity. Such concepts have been further advanced by Baker and Cornell [3] who build upon the framework of the Pacific Earthquake Engineering Research (PEER) Center to propagate the uncertainty from the model to the decision variables (e.g., losses) using FOSM methods. Other efforts extend the SAC/FEMA approach to the assessment of reinforced concrete buildings [4] or the development of decision-making tools for the conceptual design of engineering facilities [5].

Although structural reliability analysis methods have considerably evolved during the last few years (e.g., [6]) the need for new approaches to estimate uncertainty for complex nonlinear structures still exists. Monte Carlo simulation methods are powerful tools that can handle almost any problem, but they always come at the expense of a large number of computationally-intensive nonlinear response history analyses. Other approximating methods such as first and second-order reliability methods (FORM, SORM) have been successfully implemented for the calculation of safety factors in most recent design code procedures, but for structures subjected to large nonlinear deformations and transient actions, such methods are plagued by the need for a failure function [6, 7].

For earthquake engineering applications, one method to handle the aleatory uncertainty introduced by seismic loading is the Incremental Dynamic Analysis (IDA) [8]. IDA essentially requires multiple nonlinear response history analyses with a suite of ground motion records to provide a full-range performance assessment, from the early elastic limit-states to the onset of collapse. To account for other sources of uncertainty, the IDA approach can be combined with reliability analysis methods such as Monte Carlo simulation. Such methods have been pioneered by Dolsek [9] who proposed using Monte Carlo simulation with efficient Latin Hypercube Sampling (LHS) on IDA and Liel *et al.* [10] that used IDA and Monte Carlo or FOSM with a response surface approximating method to study parameter uncertainty. More recently, Vamvatsikos and Fragiadakis [11] have also discussed an IDA-based approach and the possibility of reducing the computational effort by adopting approximate, moment-estimating methods. Although such IDA-based methods are powerful, they necessitate the execution of a large number of nonlinear response history analyses and therefore are beyond the scope of many practical applications. While the above publications propose alternative approaches and discuss either implicitly or explicitly the issue of computing cost, they all use nonlinear response history analysis under multiple ground motion records. Clearly this may not be feasible at the present time for practical, non-academic, applications. Simpler analysis methods are needed that can provide estimates of the response statistics with minimum computing resources.

Given the computational obstacles, the usual practice to circumvent this problem is by

assuming ad hoc values for the dispersions caused by uncertainties, e.g. in the model properties, and either implicitly taking them into account or explicitly including them in the guidelines, as in FEMA-350. For example, Yun *et al.* [12] discuss the rationale behind the tabulated values of the FEMA-350 [1] guidelines. Evidently, the proposed parameters are semi-empirically derived from a limited number of benchmark structures. These values can be seen as reasonable placeholders that, unfortunately, in the absence of more rational and proven values, tend to become the de facto standard.

In search for a compromise, we propose a novel methodology for estimating response statistics using static pushover analysis. During the past few years, static pushover methods (SPO) have become common in the earthquake engineering practice [13, 14] and therefore this analysis approach lies in the core of the methods we are proposing. Furthermore, a single static pushover requires considerably less computational resources compared to the hundreds response history analyses of an actual multi-record IDA that are practically beyond the scope of most projects. Similarly to IDA, our method maintains a full-range performance evaluation capability using as link between SPO and IDA an $R - \mu - T$ (force reduction factor - ductility - period) relationship, known as Static Pushover to Incremental Dynamic Analysis (SPO2IDA) [15, 16]. SPO2IDA is an $R - \mu - T$ relationship that offers accurate prediction capabilities even close to collapse using, instead of bilinear elastoplastic, a multilinear approximation of the static pushover envelope. Having such a tool at our disposal we can quickly perform all the necessary simulations and obtain an estimate of the effect of uncertainty on the demand and capacity of structures. Using a nine-storey steel frame as a reference structure we will employ Monte Carlo simulation and moment-estimation techniques together with static pushover and SPO2IDA to achieve rapid evaluation of the seismic performance variability due to epistemic uncertainty in our model parameters.

2. STRUCTURAL MODELS

The structure considered is a nine-storey steel moment-resisting frame with a single-storey basement, shown in Figure 1. The frame has been designed according to 1997 NEHRP (National Earthquake Hazard Reduction Program) provisions for a Los Angeles site. We use a centerline model with nonlinear connections created at the OpenSees [17] platform. The beams are modelled with lumped-plasticity elements, thus allowing the formation of plastic hinges at the two beam ends. The columns are considered elastic, consistent with a strong-column, weak-beam design. Preliminary testing has shown that cases where column yielding occurs are isolated and therefore this choice has a negligible effect on the accuracy of model while it considerably reduces its complexity. Geometric nonlinearities have been incorporated in the form of $P - \Delta$ effects, while the internal gravity frames have been explicitly modeled (Figure 1). In effect, this is a first-mode dominated structure with a fundamental period of $T_1 = 2.35s$ and a modal mass equal to 84% of the total mass that still allows for a significant sensitivity to higher modes.

The connections are modeled using the “Hysteretic material” of the OpenSees library [17]. This is a uniaxial moment-rotation relationship that allows modelling the fracturing connections with rotational springs having moderately pinching hysteresis and a quadrilinear backbone, shown in normalised coordinates in Figure 2 (see also reference [18]). The random parameters considered refer to the properties of the quadrilinear backbone curve, which initially

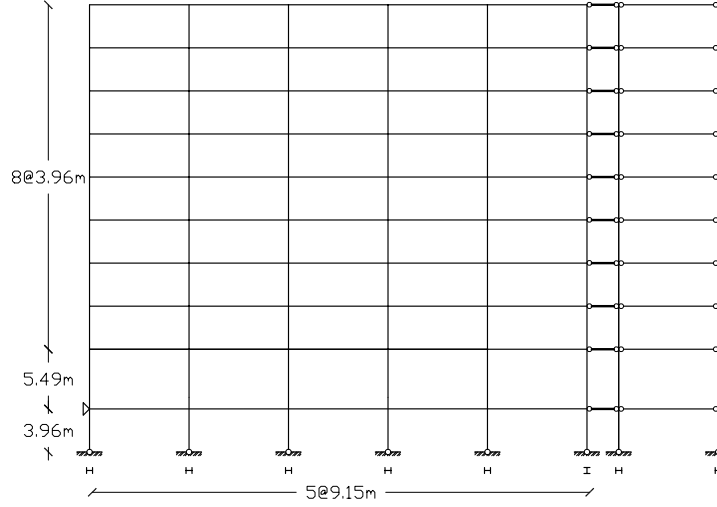


Figure 1. The LA9 steel moment-resisting frame.

Table I. Random parameters and their statistics.

	Mean	c.o.v	Lower bound	Upper bound
a_{M_y}	1.0	0.20	0.70	1.30
a_h	0.1	0.40	0.04	0.16
μ_c	3.0	0.40	1.20	4.80
a_c	-0.5	0.40	-0.80	-0.20
r	0.5	0.40	0.20	0.80
μ_u	6.0	0.40	2.40	9.60

allows for elastic behavior up to a_{M_y} times the nominal yield moment M_y , then hardens at a non-negative normalised slope of a_h and terminates at a rotational ductility μ_c . Beyond this point, a negative stiffness segment starts having a normalised slope a_c . The residual plateau appears at a normalised height r , delaying the failure of the connection until the ultimate rotational ductility μ_u . Thus to completely describe the backbone of the monotonic envelope of the hinge moment-rotation relationship, six parameters are necessary: a_{M_y} , a_h , μ_c , a_c , r and μ_u , assuming similar behavior for both positive and negative moments. This is essentially a complex backbone that is versatile enough to simulate the behavior of numerous moment-connections. Other sources of epistemic uncertainty (e.g. stiffness and/or mass uncertainty) are not examined here, although our methodology can be easily extended to those parameters also.

The backbone properties of the plastic hinges are considered as random variables and hence

are the only source of epistemic uncertainty. The parameters are modeled to be independently normally distributed with mean and coefficient of variation (c.o.v) as shown in Table I. The mean values represent best estimates of the backbone parameters, while the c.o.v values were assumed, since for most parameters there is no explicit guidance in the literature. Thus we used a c.o.v equal to 40% for all the parameters except for the yield moment where 20% was used instead. To avoid assigning the random parameters with values with no physical meaning, e.g. $a_h > 1$, or $r < 0$, their distribution is appropriately truncated within 1.5 standard deviations as shown in Table I. All distributions were appropriately rescaled to avoid the concentration of high probabilities at the cutoff points. The resulting connection model is flexible enough to range from fully-ductile, nearly elastoplastic connections (e.g. $r = 0.80$, $\mu_u = 9$) down to outright brittle cases that suddenly fracture at low ductilities (e.g. $\mu_u = 2.4$).

To account for parameter uncertainty stemming from the properties of the connections of a steel moment frame, the plastic hinge properties can be varied simultaneously for the whole structure, or individually, by applying local changes to several connections. In the later case the precise locations of the connections are randomly assigned thus assessing the global performance when the capacity of a number of connections is uncertain e.g. due to poor manufacturing or localised phenomena. Luco and Cornell [19] studied the response of moment-resisting frames with random fracturing connections typical to those of pre- and post-Northridge steel buildings. On the other end, varying together the properties of every frame connection, i.e. assuming that all have the same normalised properties, is expected to have a more pronounced effect on the response, pinpointing the influence of each of the six parameters on the global capacity. This scenario is the one we are going to adopt as it is consistent with the case where the engineer does not have sufficient data for the individual moment-rotation backbones and their spatial correlation, thus his/her model relies on empirical values and judgment.

3. PERFORMANCE EVALUATION WITH THE STATIC PUSHOVER TO INCREMENTAL DYNAMIC ANALYSIS TOOL

3.1. Incremental Dynamic Analysis

Incremental Dynamic Analysis (IDA) is a powerful analysis method that offers thorough seismic demand and capacity prediction capability [8]. It involves performing a series of nonlinear response history analyses under a multiply scaled suite of ground motion records. By selecting proper Engineering Demand Parameters (EDPs) to characterise the structural response and choosing an Intensity Measure (IM), e.g. the 5%-damped, first-mode spectral acceleration $S_a(T_1, 5\%)$, to represent the seismic intensity, we can generate the IDA curves of EDP versus IM for every record and then estimate the 16%, 50% and 84% summarised curves. The EDP typically adopted is the maximum interstorey drift, θ_{max} , that previous research has shown that is a good measure of structural damage, while other EDPs can be adopted as in cases where non-structural acceleration-sensitive damage is of interest. On the IDA curves the desired limit-states (e.g., immediate occupancy or collapse prevention according to [1]) can be defined by setting appropriate limits on the EDPs and then estimating the corresponding capacities and their probabilistic distributions. Such results combined with probabilistic seismic hazard analysis [8] allow the estimation of mean annual frequencies (MAFs) of exceeding the

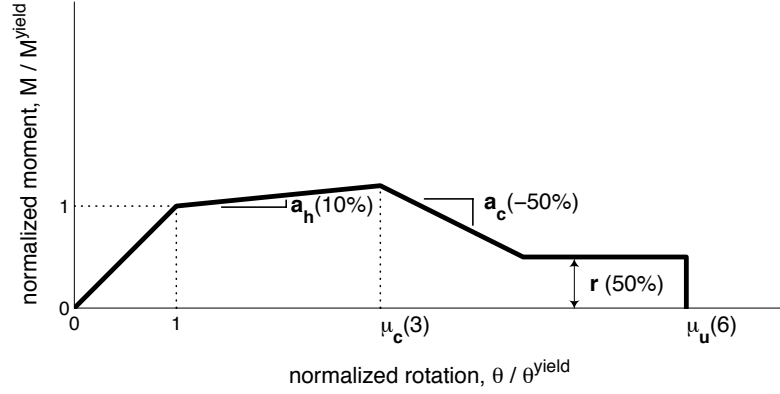


Figure 2. The moment-rotation relationship of the beam point-hinge in normalised coordinates.

limit-states (e.g. reference [20]) thus offering a direct characterization of seismic performance. Even for simple structures, IDA comes at a considerable cost, since it requires the use of multiple nonlinear response history analyses that are usually beyond the abilities and the computational resources of the average practicing engineer. Therefore, a simpler and faster alternative is always desirable.

Figure 3a shows thirty single-record IDA curves for the LA9 steel frame. Each curve has been obtained from fourteen response history analyses using the hunt-and-fill algorithm and then interpolating with appropriate splines [20]. The table of the ground motion records used for this analysis is given in reference [11]. In Figure 3a, the collapse limit-state appears at a θ_{max} value approximately equal to 0.1, signifying the initiation of the flatline branch. The thirty single-record IDAs are summarised to produce the median and the 16%, 84% percentile curves of Figure 3b. The median, or 50% fractile, provides a ‘central’ capacity curve, while the 16%, 84% percentiles give a measure of the dispersion around the median. The fractile capacities can be summarised either in terms of $S_a(T_1, 5\%)$ with respect to θ_{max} , i.e. $S_a(T_1, 5\%)|\theta_{max}$, or in terms of θ_{max} given the spectral acceleration $S_a(T_1, 5\%)$, i.e. $\theta_{max}|S_a(T_1, 5\%)$. In practice [20] and provided that a reasonably large number of records is used, both approaches are expected to yield equivalent results (Figure 3b) and therefore the final choice of the post-processing method depends on the problem at hand. In the remainder of the paper we mainly concentrate on the S_a -capacity given θ_{max} statistics, but this does not restrict our methodology since our results can be easily translated to θ_{max} -demand given the IM statistics.

3.2. Static Pushover to Incremental Dynamic Analysis (SPO2IDA)

IDA is a comprehensive, yet computer-intensive method. It is possible to approximate the results of IDA both for single and for multi-degree-of-freedom systems utilising information from the force-deformation envelope (or backbone) of the static pushover to generate the summarised 16%, 50% and 84% IDA curves [15, 16]. The prediction is based on the study of numerous SDOF systems having a wide range of periods, moderately pinching hysteresis and 5% viscous damping, while they feature backbones ranging from simple bilinear to complex quadrilinear, as shown in Figure 2. Having compiled the results into the SPO2IDA tool,

available online [21] we can get an approximate estimate of the performance of virtually any oscillator without having to perform the costly analyses, and quickly recreate the fractile IDAs. SPO2IDA is in essence an $R - \mu - T$ relationship that will provide not only central values (mean or median) but also the dispersion, due to record-to-record aleatory randomness, using only a multilinear approximation of the static pushover curve.

For SDOF structures, IDA curves can be appropriately represented in normalized coordinates of the strength reduction factor R , versus the ductility μ . The strength reduction factor R is defined as the ratio $S_a(T_1, 5\%) / S_a^{yield}(T_1, 5\%)$, where $S_a^{yield}(T_1, 5\%)$ is the $S_a(T_1, 5\%)$ value to cause first yield, while the ductility, μ , is the oscillator's displacement, δ , normalised by the yield displacement, δ^{yield} . Thus once the period and the properties of the force-deformation relationship are known for the SDOF system, SPO2IDA directly provides its median and the 16, 84% fractile demand and capacity in normalised R, μ coordinates.

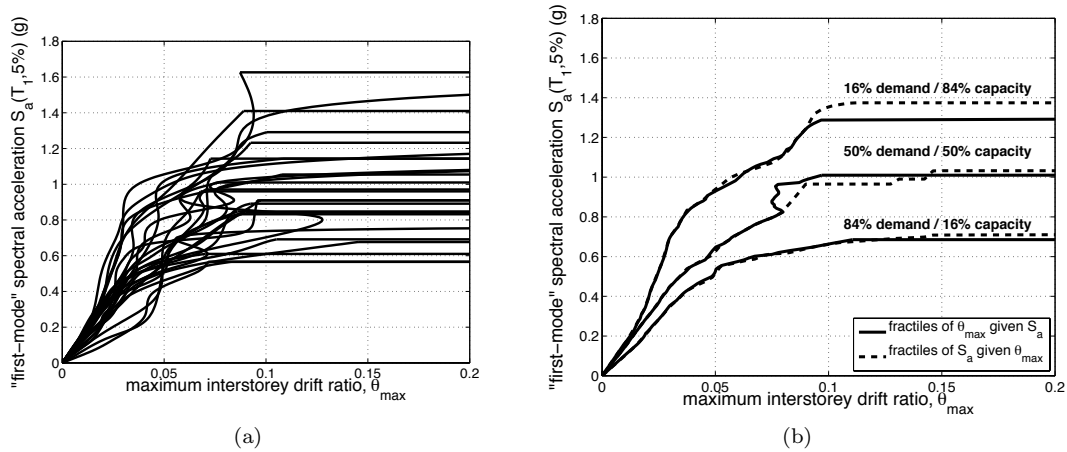


Figure 3. Incremental Dynamic Analysis (IDA) curves for the LA9 steel structure: (a) thirty single-record IDAs, and (b) summarisation of the thirty IDA curves into their fractile curves of θ_{max} given $S_a(T_1, 5\%)$, or $S_a(T_1, 5\%)$ given θ_{max} .

3.3. SPO2IDA for multi-degree of freedom systems (MDOF)

The SPO2IDA tool has been extended to first-mode dominated MDOF structures [16], enabling an accurate estimation of the fractile IDA curves even close to collapse without the need of any nonlinear response history analysis. In addition, it has been shown to only slightly increase the error in our estimation, resulting to an accuracy that can be compared to that of the actual IDA using a smaller number, e.g. ten, ordinary ground motion records. Thus SPO2IDA can approximate the summarized IDA results, offering an efficient and simple method for estimating the uncertainty associated with the limit-state capacities, given the variability in the backbone parameters of the beam plastic hinges. In the following paragraphs we explain in detail its application on our testbed structure and we propose a simplified method (compared to reference [16]) that can be used for epistemic uncertainty estimations within Monte Carlo.

The application of the SPO2IDA tool on the base-case, mean-parameter model of the LA9

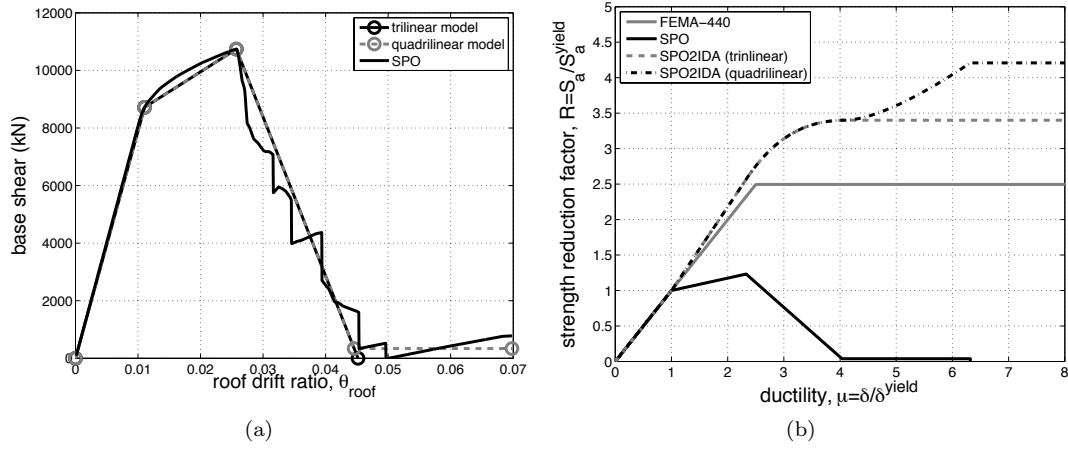


Figure 4. (a) The SPO curve for a nine-storey steel structure and its approximation with different multilinear models, (b) SPO2IDA predictions for the trilinear and the quadrilinear approximations of the SPO in R, μ coordinates.

moment-resisting steel structure is schematically shown in Figure 4. The process involves approximating the static pushover curve with a multilinear envelope to allow extracting the properties of the backbone curve (Figure 4a). The complete theoretical justification and discussion on the application of SPO2IDA on MDOF structures can be found in [16]. Typically for first-mode dominated structures, SPO2IDA allows the use of a bilinear, trilinear or full quadrilinear approximation of the structure's pushover curve. While the accuracy of the approximation rises accordingly, so does the complexity of the automated fitting algorithm to estimate the appropriate parameters, an issue that we discuss in the section that follows. For the sake of comparison, we will attempt both a trilinear and a quadrilinear fit as shown, e.g. in Figure 4a.

The choice of the lateral load pattern has a significant effect on the SPO envelope and therefore Vamvatsikos and Cornell [16] report that the proper application of SPO2IDA on MDOF structures entails the identification of the most-damaging lateral load pattern. For this realisation of the LA9 steel frame it was found that a triangular or a first-mode pattern will provide sufficiently accurate results, close to the worst-case scenario. Thus we are spared the need to search for the most damaging pattern for every realisation of the structure in the Monte Carlo simulation. In the general case, alternative lateral load patterns have to be tested for every frame realisation to find the one that seems to be the most damaging. For the methodology discussed here, this has to be performed only for the base-case, mean parameter structure.

Moreover, although SPO2IDA provides all three 16,50,84% fractile curves, we may simplify its application by using only the 50% curve together with the typical first-order assumption [22], where the base-case mean parameter model is assumed to provide the overall mean/median response and the parameter uncertainty is only considered to add variability around this mean/median. This was shown by Vamvatsikos and Fragiadakis [11] to be a viable assumption for this structure, thus, in the interest of simplicity, this will be our main proposal. Nevertheless,

the ability to compute the 16 and 84% fractiles allows the application of this method in a more general sense.

Having approximated the SPO curve, the backbone parameters can be easily extracted. Following the terminology of SPO2IDA (for a backbone description similar to that of Figure 2) the extracted parameters will be: F_y^{SPO} (instead of M_y in Figure 2), a_h^{SPO} , μ_c^{SPO} , a_c^{SPO} . For the trilinear approximation r^{SPO} is set equal to zero and μ_u^{SPO} is defined as the intersection of the horizontal axis with the descending branch, while for the quadrilinear model they are extracted from the SPO as the remaining parameters. The six parameters are then given as input to SPO2IDA to produce the median capacities shown in Figure 4b.

Figure 4b shows in $R - \mu$ coordinates the SPO2IDA-produced capacities together with the corresponding SPO. The difference between the trilinear and the quadrilinear approximation is the truncation of the tail of the SPO (Figure 4a) which results to a slight underestimation of the R capacity when the trilinear model is adopted. Figure 4b also shows the capacity predicted with a simpler code-prescribed $R - \mu - T$ relationship, such as that of the FEMA-440 guidelines [14]. For medium to long periods (typically $T_1 \geq 1$) almost every such relationship follows the equal-displacement rule and thus the ratio of R over μ is equal to one. FEMA-440 also sets an upper limit on the maximum R -value considerable, R_{max} , which adopting the notation of this paper is calculated as follows:

$$R_{max} = \mu_h^{SPO} + \frac{(\alpha_c^{SPO})^{-t}}{4} \quad (1)$$

where $t = 1 + 0.15 \ln(T_1)$. FEMA-440 uses this limit to introduce the physical bounds of the $R - \mu - T$ relationship indicating that when R_{max} is exceeded more elaborate methods of analysis need to be considered. This relationship can be considered as an alternative to SPO2IDA that can be implemented at a 30-40% underestimation in the near collapse region (Figure 4b.)

Since the capacities of SPO2IDA are in dimensionless $R - \mu$ coordinates, they need to be scaled to another pair of IM, EDP coordinates, more appropriate for MDOF systems, such as the $S_a(T_1, 5\%)$ and the maximum interstorey drift ratio θ_{max} . The scaling from $R - \mu$ to $S_a(T_1, 5\%) - \theta_{max}$ is performed with simple algebraic calculations:

$$\mathbf{S}_a(T_1, 5\%) = \mathbf{R} \cdot S_a^{yield}(T_1, 5\%) \quad (2)$$

$$\boldsymbol{\theta}_{roof} = \boldsymbol{\mu} \cdot \theta_{roof}^{yield} \quad (3)$$

where the bold font denotes a vector. Once $\boldsymbol{\theta}_{roof}$ is known, $\boldsymbol{\theta}_{max}$ can be extracted from the results of the SPO, since for every load increment the correspondence between the two EDPs is always available.

Prior to applying Equations 2 and 3 we have to determine the values of $S_a(T_1, 5\%)$ and θ_{roof} at yield. This task is trivial for SDOF systems, but it is not straightforward for MDOF structures mainly due to the effect of higher modes. Some records will force the structure to yield earlier and others later, thus yielding will always occur at different levels of $S_a(T_1, 5\%)$ and θ_{roof} . Driven by our approximation to the SPO curve, we let the yield roof drift, θ_{roof} , be defined as the apparent yield point of the multilinear approximation. This assumption is not strictly true for MDOF structures and it becomes highly accurate only if the first mode is dominant, but it is sufficient for our purpose. Therefore, the accurate estimation of $S_a^{yield}(T_1, 5\%)$ comes down to approximating the elastic “slopes” of the median IDA curves plotted with θ_{roof} as the

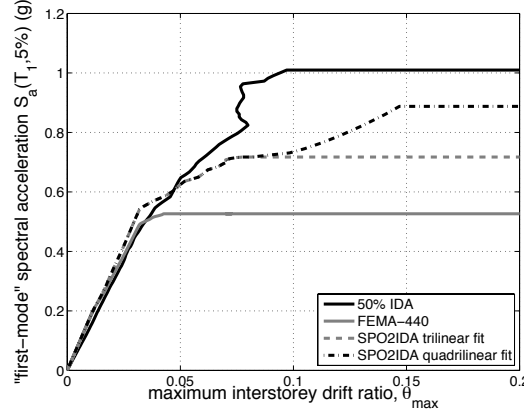


Figure 5. The approximate capacity curves of Figure 4b, plotted against the actual median IDA.

EDP. The slope, denoted as k_{roof} , is the median value obtained using elastic response history analysis with a few ground motion records, or simply by using standard response spectrum analysis. For first-mode dominated systems a quick estimate can also be obtained by employing a first-mode approximation via the roof displacement participation factor, e.g. the C_0 factor defined by the FEMA-356 [13] or FEMA-440 [14] guidelines. For example, using the target displacement equation of FEMA-356 and given that in the elastic range the coefficients C_1 , C_2 , C_3 are equal to one, the roof drift and the IDA slope k_{roof} are obtained as:

$$\theta_{\text{roof}} = \frac{\delta_{\text{roof}}}{H} = C_0 S_a \frac{T_1^2}{4\pi^2 H} g \quad (4)$$

$$k_{\text{roof}} = \frac{S_a(T_1, 5\%)}{\theta_{\text{roof}}} = \frac{4\pi^2 H}{C_0 T_1^2 g} \quad (5)$$

where H is the height of the building and g the surface gravity acceleration in appropriate units. Finally, $S_a^{\text{yld}}(T_1, 5\%)$ will be:

$$S_a^{\text{yld}}(T_1, 5\%) = k_{\text{roof}} \cdot \theta_{\text{roof}}^{\text{yld}} \quad (6)$$

As long as the first-mode dominates the response, such estimates are accurate enough for uncertainty estimation, an issue that we will discuss in a section that follows.

In summary, the process of producing an approximate IDA curve from a single static pushover run involves the following steps. Initially perform a static pushover analysis with a first-mode lateral load pattern and then approximate it either with a trilinear or a quadrilinear model. Next SPO2IDA will provide the IDA curves in normalised R, μ coordinates. The final step is scaling the IDAs to the $S_a(T_1, 5\%)$, θ_{max} coordinates. This requires the elastic slope of the actual IDA, k_{roof} , when θ_{roof} is used as the EDP. Therefore, a few linear elastic response history or response spectrum runs are need, or alternatively the approximate Equation 5 can be used. Note that in our case k_{roof} has to be calculated only once for all instances of the model since none of the uncertain parameters influences the elastic response. With the aid of Equations 2 and 6 we obtain the IDAs in $S_a(T_1, 5\%) - \theta_{\text{roof}}$ coordinates. The final IDAs are reached using the mapping between θ_{roof} and θ_{max} , available from the results of the SPO.

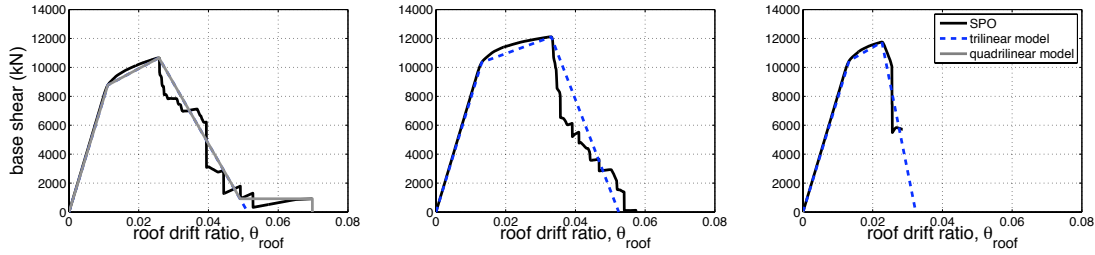


Figure 6. Different SPO curves and their multilinear approximation.

For the SPO curve of Figure 4, the median IDA obtained with SPO2IDA and the actual IDA curve using thirty ordinary ground motion records [11] are shown in Figure 5. For our model, the error in the procedure is typically 10–20%, while the computing time comes down from 2–3 hours required for a single IDA to just a couple of minutes for SPO2IDA, approximately two orders of magnitude less. It is worthwhile to note that compared to the quadrilinear pushover approximation, the trilinear curve slightly biases our IDA results towards lower S_a -capacities, the reason being our truncating of the tail of the pushover as shown in Figure 4a. The FEMA-440 relationship is accurate enough only for low elastic and nearly-elastic $S_a(T_1, 5\%)$ intensities thus leaving more elaborate relationships, such as SPO2IDA, to be the only alternative when approximate capacity estimations are sought for high intensity, near-collapse levels. The small discrepancies in the elastic range that appear between the four curves of Figure 5 are actually a direct by-product of the elastic IDA-slope determination process. While the FEMA-440 curve seems to be more accurate, there are always small implementation details that can swing these minor differences either way.

3.4. Fitting the SPO curves

The fitting of a multilinear model on the SPO is not a trivial issue, especially when it has to be performed without supervision within a Monte Carlo scheme. This issue has already received attention as it is discussed in the guidelines [13, 14] to serve purposes seemingly different to those of our study. For example the FEMA-356 [13] guidelines propose the fitting of a bilinear curve on the force-displacement relationship to assist calculating the effective stiffness and the yield strength of the whole structure. The effective stiffness is taken as the secant stiffness calculated at a base shear equal to 60% of the effective yield strength, while the slope of the post-elastic segment is chosen so that balance is achieved between the areas above and below the SPO data. The FEMA-440 [14] guidelines discuss the fitting of the strength degrading segment with a line of negative slope α_c . It is suggested to separate the effect of $P - \Delta$ phenomena by repeating the analysis with and without including them and performing the fitting for each case to obtain the slopes $\alpha_{P-\Delta}, \alpha_{w/o, P-\Delta}$. Then the final slope is calculated as the weighted sum: $\alpha_c = \alpha_{P-\Delta} + \lambda(\alpha_{w/o, P-\Delta} - \alpha_{P-\Delta})$, where λ is taken 0.2 for a near-field site or 0.8 otherwise. It is evident that the above fitting approaches require engineering judgment and are sensitive to non-objective decisions. To serve our purposes the fitting has to be performed within a software tool and thus we need to develop a generally-applicable and robust algorithm that can fit a multilinear curve on the SPO curve.

The fitting of a trilinear or a quadrilinear model on the SPO depends primarily on the properties of the SPO curve. Figure 6 shows three different SPO curves that the fitting algorithm should be able to handle. The plot in the left is the most common where both trilinear and quadrilinear models can be fitted, contrary to the case in the middle where the original SPO does not have a residual plateau and therefore only a trilinear curve can be fitted. Finally, the right plot shows a case where the SPO is abruptly terminated due to numerical non-convergence, signifying a very brittle structure (assuming the analysis has been carefully performed). All such cases need to be handled efficiently.

In our implementation, the fitting of the SPO is performed in two distinct phases. The first phase refers to fitting the elastic and the post-elastic segment until the point where ‘capping’ occurs, i.e. the point where the negative segment is initiated. In the second phase we fit the ‘post-capping’ segment with slope α_c and the residual strength plateau with ordinate r (Figure 2). Previous research [11, 16] has revealed that the yield strength and the post elastic stiffness, $\alpha_h K_{el}$, seem to have a significant effect at the SPO-level, but when IDA is performed the sensitivity is small. Therefore the fitting process is simple in this phase and can be done by obtaining the slopes α_{el} and α_h of the elastic and the post-elastic segment, respectively, and define the yield point as the intersection of the two lines. Alternatively the yielding point can be defined as the point where the tangent slope reaches for the first time a given percentage (say 50%) of the initial elastic. In our study, both approximations will yield almost equivalent SPO2IDA results.

The post-capping stiffness, α_c , and the height of the residual plateau, r , are more difficult to capture, while our results are more sensitive to those parameters. Again two alternative strategies have been tested. In the first alternative we perform least-square fitting on the points between the capping point and the first point of the SPO with base shear lower than an reasonably-chosen value, say 30%, of the yield strength. Care needs to be taken to scale the coordinates of the SPO so that the least-square line passes through the capping point. In other words, if V^c and θ_{roof}^c are the coordinates of the capping point and K_{el} the initial elastic stiffness, the fitted line can be expressed as $(V - V^c) = a_c K_{el} (\theta_{roof} - \theta_{roof}^c)$. The residual strength, r , is obtained by finding the horizontal line that balances the areas between the branch with negative slope a_c and the remaining points of the SPO. For a quadrilinear approximation a second alternative is also available. In this case an iterative process that passes through every point of the SPO that lies beyond the capping point is initiated. Trial a_c and r values are defined by the coordinates of the trial point and the areas above and below the approximating lines are calculated. The point where best balance is achieved defines the intersection point of the descending and the horizontal branch. Note that when this process is followed, the abscissas and the ordinates of the SPO need to be normalised by their maximum values to achieve efficient fitting. In our case, both procedures were found equally efficient, while for our implementation we have adopted the first option. Contrary to FEMA-440 we found that there is no need to separate the loss in strength caused by $P - \Delta$ effects and the component in-cycle strength degradation, since our SPO2IDA tool treats both sources of nonlinearity equally.

4. METHODOLOGY

In order to accurately calculate the performance statistics of a structure using static pushover methods, we will employ an approach based on the Monte Carlo (MC) simulation with Latin Hypercube Sampling (LHS), conceptually following the idea proposed by Dolsek [9]. As simpler and less resource-demanding alternatives we propose methods that rely on moment-estimating techniques such as Rosenblakth's $2K+1$ point estimate method (PEM) [?] and the first-order, second-moment method (FOSM) [6, 7].

4.1. Monte Carlo Simulation with Latin Hypercube Sampling (LHS)

Using the Monte Carlo (MC) simulation on top of SPO2IDA we are able to quickly obtain a sufficient sample of IDA curves which can be post-processed to provide the required response statistics. Since we are interested primarily in the mean and the dispersion of the capacity, the MC method can be combined with the Latin Hypercube Sampling (LHS) method [24] to ensure improved accuracy with only a few simulations compared to classic random sampling. As previously discussed, the random variables are the six parameters that fully describe the backbone of the plastic hinge moment-rotation relationship (Figure 2) and they are varied concurrently throughout the structure. Using their distribution properties (Table I) we obtain N_{LHS} samples with the aid of the algorithm of Iman and Conover [25] to ensure zero correlation among the six variables. Each of the N_{LHS} realizations of the LA9 frame is subjected to a pushover analysis and then the SPO2IDA tool is utilised to finally obtain N_{LHS} median IDA realizations, as discussed in the previous section.

According to Iman [26], if n^3 simulations are required to estimate the variation of a *linear* function with a given level of confidence using Monte Carlo with random sampling, then Monte Carlo with LHS sampling will achieve an equivalent estimate with the same confidence after only n simulations. For nonlinear functions, there are no closed-form relationships, but still LHS would normally require less simulations than random sampling, as long as the sample size n is large compared to the number of variables K . When the response statistics of buildings subjected to seismic actions are sought, the accuracy of LHS for our nonlinear structure is expected to be close to that of a linear system, since the localized nature of nonlinearity (beam-hinging) reduces changes in the stiffness matrix to a minimum. Therefore, the degree of nonlinearity of the problem is actually quite small. In any case, as discussed in [11] a sample size of $N_{\text{LHS}} = 200$ Monte Carlo simulations with latin hypercube sampling is expected to provide a close estimate of the response statistics of the problem considered here, although smaller sample sizes may have been also adequate [9]. A parametric investigation of the required number of Monte Carlo simulations, N_{LHS} , is presented in the last section of the paper.

In our development we are interested in estimating a central value and a dispersion for the S_a -values of capacity for a given limit-state defined at a specific value of θ_{max} . As a central value we use the median of the $S_a(T_1, 5\%)$ -capacities given θ_{max} , $\Delta_{S_a|\theta_{\text{max}}}$, while the dispersion caused by the uncertainty in the median capacity will be characterised by its β -value, [2], i.e. the standard deviation of the natural logarithm of the median S_a -capacities conditioned on θ_{max} : $\beta_U = \sigma_{\ln S_a|\theta_{\text{max}}}$. In terms of the work of Jalayer [22] we essentially adopt the IM-based method of estimating the mean annual frequency of limit-state exceedance.

Thus, if $\ln S_{a,50\%}^j$, $j = 1, \dots, N_{\text{LHS}}$, are the median S_a -capacities for a given value of θ_{max} and $\overline{\ln S_{a,50\%}}$ is the mean of their natural logarithm, we can obtain the overall median and

dispersion, β_U , as:

$$\Delta_{S_a} = \text{med}_j \left(S_{a,50\%}^j \right) \quad (7)$$

$$\beta_U = \sqrt{\frac{\sum_j \left(\ln S_{a,50\%}^j - \overline{\ln S_{a,50\%}} \right)^2}{N_{LHS} - 1}} \quad (8)$$

where “med_j” is the median operator over all indices j .

According to the work of Cornell *et al.* [2], such an estimate of the response dispersion due to epistemic uncertainty can be combined with the dispersion due to record-to-record aleatory randomness with a square-root-sum-of-squares (SRSS) rule to provide the total variability:

$$\beta_{RU} = \sqrt{\beta_R^2 + \beta_U^2} \quad (9)$$

This assumption has seen much use and it has been shown to work reasonably well for this structure [11]. Alternatively, one could take advantage of SPO2IDA’s ability to provide both the central value and the dispersion of demand and capacity due to aleatory randomness to allow a more precise estimation of the overall variability β_{RU} . By assuming a lognormal distribution of capacity S_a given θ_{max} , the 50% IDA will provide the median while the 16 and 84 fractile IDAs allow us the estimation of its dispersion, for every sample and every value of θ_{max} . Thus, for every sample structure we can draw 30 (or more) random IDA curves according to the distribution properties prescribed by the 16, 50 and 84% percentiles. Then we can pool together the results from all $N_{LHS} = 200$ samples and compute the overall median and β_{RU} from the $30 \times 200 = 6000$ single-record $S_a|\theta_{max}$ IDA curves, much in the way that was done by Vamvatsikos and Fragiadakis [11] for the actual IDA runs. As the results will show, this level of sophistication is not necessary for our case-study.

4.2. Approximate Moment Estimation

A simpler alternative to performing Monte Carlo simulation is the use of moment-estimating methods to approximate the variability in the IDA results. Such methods are typically based on a small number of runs for appropriately perturbed versions of the structural model obtained with the mean parameter values. Using functional approximations or moment-matching, such schemes manage to propagate uncertainty from the parameters to the final results using only a few IDA runs. Specifically in this study we investigate the point estimate method (PEM) of Rosenlueth [?] and the first-order, second-moment method (FOSM) [7, 6]. Other methods that probably could be adopted, but have not been examined here, are response surface methods (e.g. [10]), or moment matching [27]. For uncorrelated and unskewed random variables, both PEM and FOSM need only two IDA evaluations per parameter, spaced one standard deviation away from the base-case mean structural model obtained using the mean parameter values. Thus to calculate Δ_{S_a} and β_U conditional on θ_{max} we need only $2K + 1 = 13$ simulations for a problem with $K = 6$ random variables.

While both methods are geared towards estimating the mean and the standard deviation of a function, they can be made to produce median and β -dispersion estimates. We only need to apply them to the $\ln S_a(T_1, 5\%)$ values rather than $S_a(T_1, 5\%)$. Then PEM and FOSM will provide the mean of the natural logarithm of $S_a(T_1, 5\%)$ and its standard deviation. The latter is exactly the definition of β_U while if we take the exponential (exp) of the former and assuming

that lognormality holds, we will get an approximation of the median $S_a(T_1, 5\%)$. Although the description of both methods can be found in standard textbooks the reader is advised to follow the implementation described in Reference [11], as there may be several misunderstandings or errors when such methods are adopted in a lognormal setting.

5. NUMERICAL RESULTS

To test the validity of the approximating procedures we first applied Monte Carlo simulation using an actual multi-record IDA with thirty ordinary records on the nine-storey, steel moment-resisting frame of Figure 1. Therefore, we have obtained the exact seismic performance metrics in IDA-terms of $N_{\text{LHS}} = 200$ realizations of the nine-storey frame. The response statistics obtained with the actual IDA are considered as a reference solution that our approximate SPO-based estimations have to comply with. The Table of ground motion records adopted can be found in Reference [11].

Figure 7a shows the $N_{\text{LHS}} = 200$ static pushover curves for the different realizations of the steel frame. The ultimate capacity varies between 7000 and 15000kN and yielding practically occurs for θ_{roof} values between 0.01 and 0.02. Significant scatter seems to exist in the initiation of the negative branch, while the negative slope itself does not seem to vary considerably. Based on the established connection between pushover and IDA, these observations lead us to expect a significant post-yield scatter of the IDA results.

Figure 7b shows the median IDAs that compare to the approximate IDAs generated with the SPO2IDA tool and are shown in Figure 8. Similarly to the median curves of Figure 5, the SPO2IDA curves are smoother than the actual IDA because of the simple backbones and the smooth parametric equations used in the SPO2IDA tool for both the trilinear and the quadrilinear approximations of Figure 8. For both SPO2IDA approximations the horizontal flatline branch of the ultimate S_a -capacities varies similarly between 0.4g and 1.2g and is practically always initiated beyond $\theta_{\text{max}} = 0.07$. On average, yielding takes place for θ_{max} values between 0.03 and 0.08, both for the IDA and the SPO2IDA results. While the scatter is similar between IDA and SPO2IDA, the central S_a values are somewhat higher for IDA, an observation that seems to be slightly demoted when the quadrilinear approximation is used. Furthermore, compared to the trilinear model the IDAs of the quadrilinear approximation show a slower transition from the initial linear elastic slope to the ultimate capacity flatline.

The IDA and SPO2IDA curves of the Monte Carlo simulation are post-processed to provide the overall median Δ_{S_a} , and the β_U -dispersion conditional on θ_{max} . Figure 9 shows the median S_a -capacities conditional on the limit-state, θ_{max} , where the black lines correspond to the capacities obtained using Monte Carlo simulation and the gray lines were derived with the approximating PEM and FOSM methods. Figure 9a corresponds to the median obtained with the trilinear model and Figure 9b to the quadrilinear approximation. When Monte Carlo simulation is used on top of SPO2IDA (MC_{SPO2IDA}) the conditional median, Δ_{S_a} , is very close to that of the actual IDA for the every limit-state, until $\theta_{\text{max}} = 0.09$, while for higher θ_{max} values the agreement is still quite satisfactory for both models. Approaching the collapse limit-states (large θ_{max} values), the error on $\Delta_{S_a|\theta_{\text{max}}}$ remains constant and approximately equal to 16% for the trilinear model, while the quadrilinear model slightly overestimates the capacity by 6%. For the early and intermediate limit-states (small and intermediate θ_{max} values), combining PEM and FOSM with SPO2IDA seems to provide a prediction for the

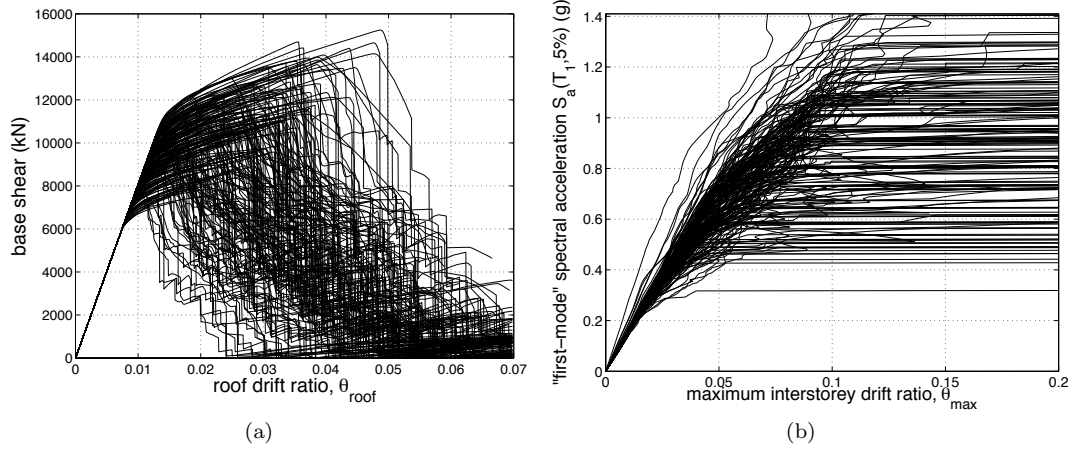


Figure 7. (a) $N_{LHS}=200$ static pushover curves for the LA9 nine-storey steel frame, (b) $N_{LHS}=200$ median response curves obtained through IDA.

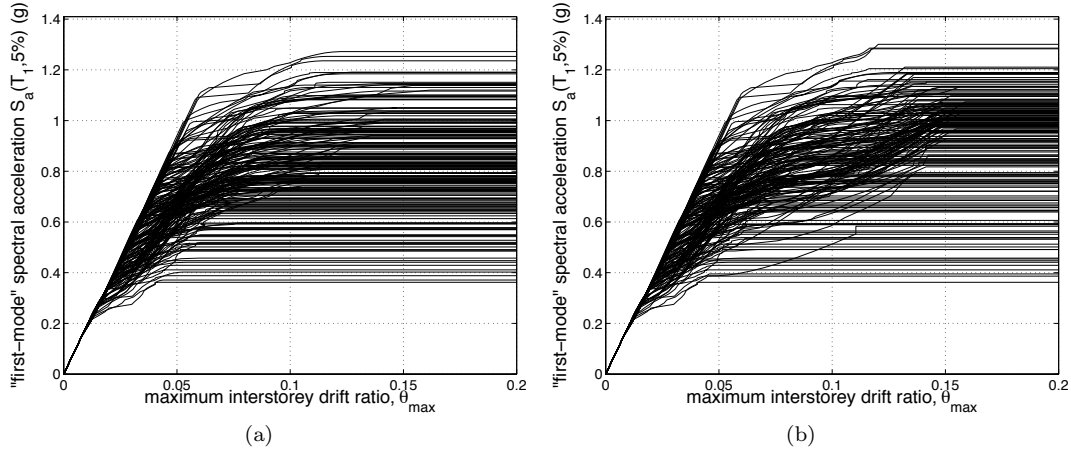


Figure 8. $N_{LHS}=200$ IDA curves obtained through SPO2IDA using: (a) a trilinear model, and (b) a quadrilinear model.

median capacities practically identical to that of MC_{IDA} and $MC_{SPO2IDA}$. However, for limit-states with $\theta_{max} \geq 0.1$, the prediction of the trilinear approximation with PEM and FOSM slightly biases the median to smaller capacities, while the quadrilinear model underestimates the median as approaching collapse. For both models, the moment-estimating methods seem to slightly fluctuate, e.g. the trilinear for θ_{max} values in the 0.04–0.08 range, implying that the estimations of the PEM and the FOSM are less numerically stable compared to those of the Monte Carlo. This numerical behaviour also seems to explain of the error of the quadrilinear model for $\theta_{max} \geq 0.1$. However, for several applications, moment-estimating methods require a smaller number of simulations, thus often justifying their use over the Monte Carlo approach.

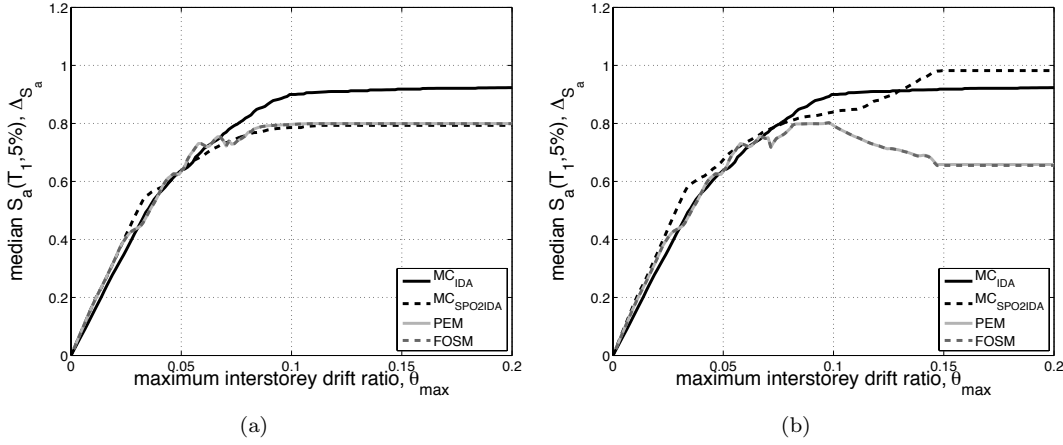


Figure 9. Conditional median of S_a given θ_{\max} estimated by Monte Carlo on IDA and SPO2IDA versus PEM and FOSM using: (a) a trilinear and (b) a quadrilinear approximation of the SPO.

Figures 10(a-d) show the dispersion β_U of the $S_a(T_1, 5\%)$ -capacities conditioned on θ_{\max} for the two approximating models. As in the case of the medians, the moment-estimating methods also exhibit some numerical problems (Figures 10a,b). Since for the β -dispersion this effect is more pronounced, we chose to smoothen those curves (Figures 10c,d) using a non-parametric locally weighted regression (LOESS) technique with a coarse span for the moving average [28], as also discussed in [11]. Within many practical applications the agreement of the methods proposed is quite satisfactory for the whole range of θ_{\max} values even when approaching collapse, regardless of the approximation of the SPO. More specifically, for the trilinear model the dispersion at collapse was found close to 0.24 with the $MC_{SPO2IDA}$ approach and 0.29 with the actual IDA, thus resulting to a 17% error, while for the quadrilinear model the dispersion was found equal to 0.26, at an error of only 10%. Both figures show that the $MC_{SPO2IDA}$ slightly overestimates β_U for θ_{\max} lower than 0.07, and underestimates it beyond 0.1. PEM and FOSM for θ_{\max} values beyond 0.7 provide β -dispersion estimates similar to that of $MC_{SPO2IDA}$, underestimating the MC_{IDA} by almost 15% for the trilinear model, while the quadrilinear model achieved a close estimation near collapse and an accuracy similar to the previous methods for θ_{\max} between 0.08 and 0.12. Both moment-matching methods can be seen as approximations to the $MC_{SPO2IDA}$ curve, rather than the MC_{IDA} . Therefore, the unsmoothed data of Figures 10a,b correctly oscillate around the $MC_{SPO2IDA}$ curve for the θ_{\max} values less than 0.07, while the smoothed data appear to be closer to the MC_{IDA} , but this is only due to the coarse span of the LOESS filter.

The accuracy observed in Figure 10 can be partially explained by the small error on the prediction of the median ΔS_a curves (Figures 5,9), which practically remains constant for every simulation and was found to be of the order of 10–20%. Since the error in the prediction of the median IDA is relatively consistent from sample to sample, the methods proposed are particularly suitable for calculating the dispersion due to epistemic uncertainty, β_U , which normally necessitates more simulations than those required for the median. For example, the elastic slope of the base-case IDA, k_{roof} , (Equation 2) was found approximately equal to 20g

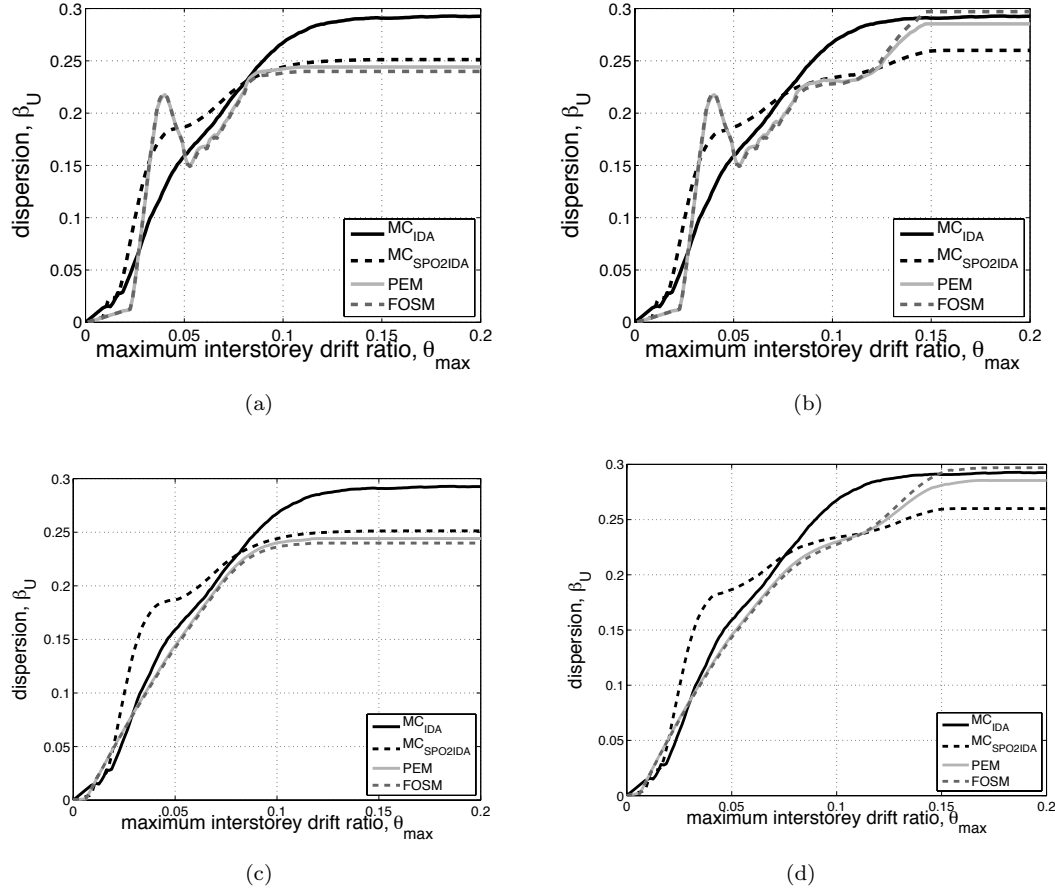


Figure 10. Conditional β -dispersion of S_a given θ_{\max} estimated with Monte Carlo on IDA and SPO2IDA versus PEM and FOSM using: (a) trilinear model, unsmoothed, (b) quadrilinear model, unsmoothed, (c) trilinear model, smoothed, (d) quadrilinear model, smoothed. The smoothing is applied only to the PEM and the FOSM methods.

using elastic response history analysis, while the slope calculated with the aid of Equation 4 is equal to 25g. While in this simplification there is an obvious bias that seriously affects the median (Figure 11a), its consistency over all samples conceals itself on the estimate of the dispersion (Figure 11b). Thus, adopting the first-mode approximate value and a trilinear model will result to overestimating the median S_a -capacities for the whole range of θ_{\max} values, while the estimation of the β -dispersion values is practically unaffected. The findings were similar when the quadrilinear model was adopted instead.

Another issue addressed here is the number of latin hypercube samples required for the Monte Carlo method to estimate the median Δ_{S_a} and the β_U -dispersion. We use our trilinear SPO2IDA approximation and with the aid of the Iman and Conover algorithm [25] we generate three different samples with $N_{LHS}=200, 50$ and 12. Figure 12 shows the estimations obtained

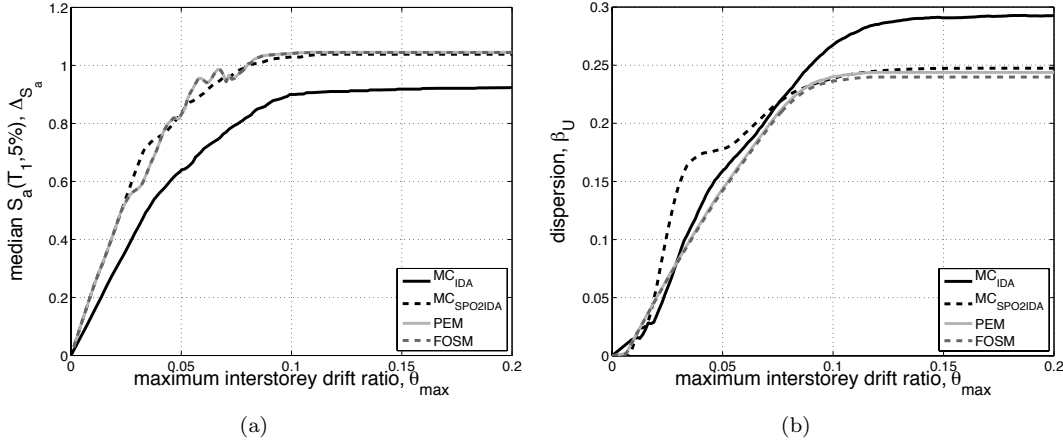


Figure 11. (a) Conditional median and (b) conditional β -dispersion values using the first-mode estimate of Equation 4 for k_{roof} . Compared to Figure 9 the mean is overestimated, while the estimate of the dispersion is not affected.

for the different sample sizes. It seems that all three samples provide sufficient estimations for the median, while for the β_U -dispersion the 200 samples give a slightly better prediction. Therefore, Figure 12 indicates that 12 samples will yield accuracy close to that of the 200 samples, and therefore the benefit of $N_{LHS}=200$ is rather small. If this observation holds for any $N_{LHS}=12$ sample, there would be no need for any moment estimating method since MC_{SPO2IDA} is more stable and requires the same number of simulations. To investigate if this is indeed the case, we generated 50 alternative suites of each of the three N_{LHS} sample sizes and we calculated the 90% confidence intervals for the prediction of the conditional median ΔS_a and the β_U -dispersion, using the empirical distribution of the data. Figure 13 shows the 90% confidence intervals for the median ΔS_a and β -dispersion when different sample sizes are adopted. For the median, the 12 samples seem to be sufficient, but certainly the prediction is not as stable as that of the 200 samples. However, for the β_U -dispersion it is clear that the 12 simulations are not sufficient and thus the successful prediction of Figure 12b was merely a coincidence.

6. CONCLUSIONS

An innovative approach has been presented to propagate the epistemic uncertainty from the model parameters to the actual seismic performance of a structure, providing inexpensive estimates of the response parameters of the limit-state capacities. The methodology proposed has been applied on a nine-storey, steel moment-resisting frame with beam-column connections having quadrilinear backbones that are fully described by six non-deterministic parameters. Monte Carlo simulation with latin hypercube sampling and moment-estimating techniques are adopted on top of the Static Pushover to Incremental Dynamic Analysis (SPO2IDA) tool. SPO2IDA provides computationally inexpensive full-range performance estimations,

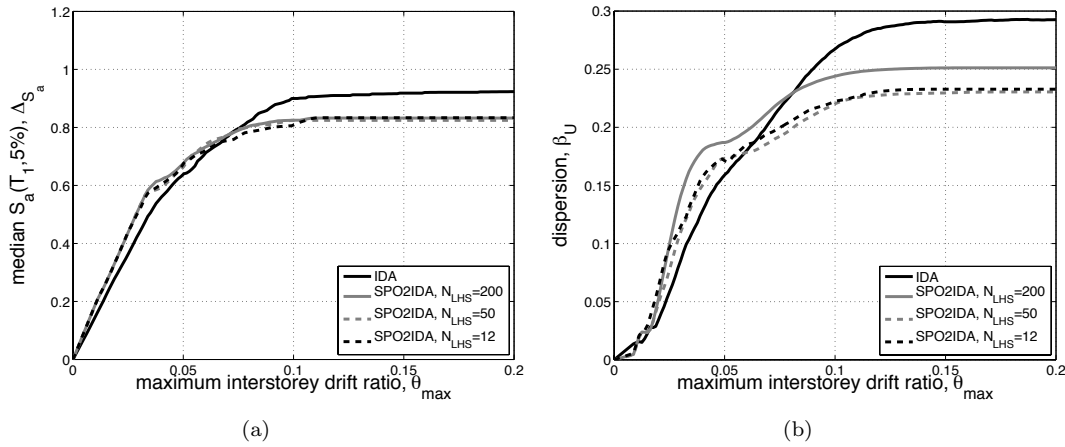


Figure 12. (a) Conditional median and (b) conditional β -dispersion values using different LHS sample sizes.

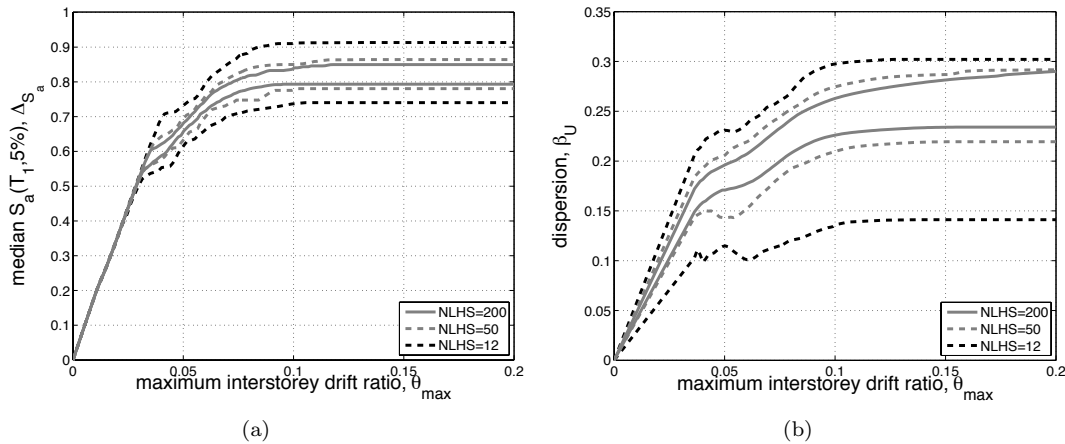


Figure 13. 90% confidence intervals for: (a) conditional median and the (b) conditional β -dispersion values using different LHS sample sizes.

approximating the time-consuming IDA. The main findings of the study are:

- The SPO2IDA tool exploits the information contained in a static pushover capacity curve and provides a reliable link between SPO and IDA that can be exploited to obtain useful response statistics for systems with uncertain parameters.
- Moment-estimating techniques require a minimum number of simulations, perturbing each random variable above and below its mean. Although the Monte Carlo simulation is combined with latin hypercube sampling to ensure good accuracy within a few simulations, the number of simulations required is considerably larger compared to that of moment-estimating methods. Still, the computing cost of MC on SPO2IDA is affordable

almost for every practical application, since each simulation corresponds to a single static pushover run.

- Combining Monte Carlo simulation and latin hypercube sampling with SPO2IDA yields close estimates for the median Δ_{S_a} capacities, only slightly under- or over- estimating them when approaching the collapse limit-states. The β -dispersion values of the S_a -capacities are also successfully approximated with only a small error for the higher limit-states.
- Moment-estimating techniques, such as PEM and FOSM, yield equivalent estimations to those of Monte Carlo on SPO2IDA, the PEM being only marginally more accurate. Compared to the Monte Carlo method they provide similar estimations for both the median Δ_{S_a} and the β -dispersion at the expense of only a few static pushover runs. Still, they are prone to numerical difficulties, in our case necessitating the use of smoothing to stabilise their results.
- For the multilinear approximation of the SPO either a trilinear or a quadrilinear model can be adopted. Both models will yield practically equivalent results, in our case the former being more stable but having the tendency to bias the predictions to lower capacities or smaller β -dispersion values.
- The number of latin hypercube samples N_{LHS} required to obtain the response statistics with sufficient confidence, depends on the problem at hand. Still, even for our simple case study with 6 random variables, only relatively large sample sizes, e.g. $N_{LHS} \geq 50$, can safeguard the accuracy of Monte Carlo.

The above findings may differ for problems with different building properties, uncertain parameters, or EDPs. However, the methodology discussed is general in scope and when adjusted to the problem at hand is able to provide results comparable to those of the Monte Carlo on actual IDA, at only a fraction of the cost. All in all, the proposed tool is an excellent resource for approximate estimation of the seismic performance of structures having uncertain system properties, for the first time providing specific results for each limit-state that can be used in the place of the generic, code-prescribed values.

REFERENCES

1. FEMA-350. *Recommended Seismic Design Criteria for New Steel Moment-Frame Buildings*. Federal Emergency Management Agency, Washington DC 2000.
2. Cornell C, Jalayer F, Hamburger R, Foutch D. Probabilistic basis for 2000 SAC/FEMA steel moment frame guidelines. *Journal of Structural Engineering* 2002; **128**(4):526–533.
3. Baker J, Cornell C. Uncertainty propagation in probabilistic seismic loss estimation. *Structural Safety* 2008; **30**(3):236–253.
4. Lupoi G, Lupoi A, Pinto P. Seismic risk assessment of RC structures with the "2000 SAC/FEMA" method. *Journal of Earthquake Engineering* 2002; **6**(4):499–512.
5. Krawinkler H, Zareian F, Medina R, Ibarra L. Decision support for conceptual performance-based design. *Earthquake Engineering and Structural Dynamics* 2006; **35**(1):115–133.
6. Pinto P, Giannini R, Franchin P. *Seismic Reliability Analysis of Structures*. IUSS Press: Pavia-Italy, 2004.
7. Melchers R. *Structural Reliability Analysis and Prediction*. John Wiley, 2002.
8. Vamvatsikos D, Cornell C. Incremental dynamic analysis. *Earthquake Engineering & Structural Dynamics* 2002; **31**(3):491–514.
9. Dolsek M. Incremental dynamic analysis with consideration of modeling uncertainties. *Earthquake Engineering and Structural Dynamics* 2008; doi:10.1002/eqe.869.
10. Liel A, Haselton C, Deierlein G, Baker J. Incorporating modeling uncertainties in the assessment of seismic collapse risk of buildings. *Structural Safety* 2009; **31**(2):197–211.

11. Vamvatsikos D, Fragiadakis M. Incremental Dynamic Analysis for seismic performance uncertainty estimation. *Earthquake Engineering and Structural Dynamics* 2009; doi:10.1002/eqe.935.
12. Yun SY, Hamburger R, Cornell C, Foutch D. Seismic performance evaluation for steel moment frames. *Journal of Structural Engineering* 2002; **128**(4):534–545.
13. FEMA-356. *Prestandard and commentary for the seismic rehabilitation of buildings*. Federal Emergency Management Agency, Washington DC 2000.
14. FEMA-440. *Improvement of Nonlinear Static Seismic Analysis Procedures*. Federal Emergency Management Agency, Washington DC 2005.
15. Vamvatsikos D, Cornell C. Direct estimation of the seismic demand and capacity of oscillators with multi-linear static pushovers through Incremental Dynamic Analysis. *Earthquake Engineering and Structural Dynamics* 2006; **35**(9):1097–1117.
16. Vamvatsikos D, Cornell C. Direct estimation of seismic demand and capacity of multidegree-of-freedom systems through incremental dynamic analysis of single degree of freedom approximation. *Journal of Structural Engineering* 2005; **131**(4):589–599.
17. McKenna F, Fenves G. *The OpenSees Command Language Manual*. 1.2. edn. 2001.
18. Ibarra L, Medina R, Krawinkler H. Hysteretic models that incorporate strength and stiffness deterioration. *Earthquake Engineering and Structural Dynamics* 2005; **34**(12):1489–1511.
19. Luco N, Cornell C. Effects of connection fractures on SMRF seismic drift demands. *Journal of structural engineering New York, N.Y.* 2000; **126**(1):127–136.
20. Vamvatsikos D, Cornell C. Applied Incremental Dynamic Analysis. *Earthquake Spectra* 2004; **20**(2):523–553.
21. Vamvatsikos D. SPO2IDA software for short, moderate and long periods 2002. URL http://blume.stanford.edu/pdffiles/Tech%20Reports/TR151_spo2ida-allt.xls, [Jan 2007].
22. Jalayer F. Direct probabilistic seismic analysis: Implementing non-linear dynamic assessments. PhD Dissertation, Department of Civil and Environmental Engineering, Stanford University, Stanford, CA 2003. URL <http://www.stanford.edu/group/rms/Thesis/FatemehJalayer.pdf>, [Oct 2008].
23. Rosenblueth E. Point estimates for probability. *Applied Mathematical Modelling* 1981; **5**:329–335.
24. McKay M, Conover W, Beckman R. A comparison of three methods for selecting values of input variables in the analysis of output from a computer code. *Technometrics* 1979; **21**(2):239–245.
25. Iman R, Conover W. A distribution-free approach to inducing rank correlation among input variables. *Communication in Statistics Part B: Simulation and Computation* 1982; **11**(3):311–1334.
26. Iman R. *Latin Hypercube Sampling*. In: Encyclopedia of Statistical Sciences, Wiley: New York, 1999. DOI: 10.1002/0471667196.ess1084.pub2.
27. Ching J, Porter K, Beck J. Propagating uncertainties for loss estimation in performance-based earthquake engineering using moment matching. *Structure and Infrastructure Engineering* 2009; **5**(3):245–262.
28. Cleveland WS. Robust locally weighted regression and smoothing scatterplots. *Journal of the American Statistical Association* 1979; **74**:829–836.